Development 136, 3757-3766 (2009) doi:10.1242/dev.042135

Mitochondrial protein Preli-like is required for development of dendritic arbors and prevents their regression in the *Drosophila* sensory nervous system

Asako Tsubouchi[1], Taiichi Tsuyama[1], Makio Fujioka[2], Haruyasu Kohda[2], Keiko Okamoto-Furuta[2], Toshiro Aigaki[3] and Tadashi Uemura[1,*,†]

Dynamic morphological changes in mitochondria depend on the balance of fusion and fission in various eukaryotes, and are crucial for mitochondrial activity. Mitochondrial dysfunction has emerged as a common theme that underlies numerous neurological disorders, including neurodegeneration. However, how this abnormal mitochondrial activity leads to neurodegenerative disorders is still largely unknown. Here, we show that the *Drosophila* mitochondrial protein Preli-like (Prel), a member of the conserved PRELI/MSF1 family, contributes to the integrity of mitochondrial structures, the activity of respiratory chain complex IV and the cellular ATP level. When Prel function was impaired in neurons in vivo, the cellular ATP level decreased and mitochondria became fragmented and sparsely distributed in dendrites and axons. Notably, the dendritic arbors were simplified and downsized, probably as a result of breakage of proximal dendrites and progressive retraction of terminal branches. By contrast, abrogation of the mitochondria transport machinery per se had a much less profound effect on the arbor morphogenesis. Interestingly, overexpression of Drob-1 (Debcl), a *Drosophila* Bax-like Bcl-2 family protein, in the wild-type background produced dendrite phenotypes that were reminiscent of the *prel* phenotype. Moreover, expression of the Drob-1 antagonist Buffy in *prel* mutant neurons substantially restored the dendritic phenotype. Our observations suggest that Prel-dependent regulation of mitochondrial activity is important for both growth and prevention of breakage of dendritic branches.

KEY WORDS: *Drosophila*, Preli, Dendrite, Mitochondria, Neurodegeneration

INTRODUCTION

Mitochondria are important for multiple cellular events such as ATP production, Ca^{2+} regulation, axonal and dendritic transport of organelles, and the release and re-uptake of neurotransmitters at synapses (Detmer and Chan, 2007). Mitochondria in most healthy cells exist as tubules of variable size and undergo dynamic morphological changes that depend on the balance of fusion and fission. This fusion-fission cycle ensures mixing of metabolites and mitochondrial DNA and influences organelle shape and bioenergetics functionality (Chan, 2006b; Okamoto and Shaw, 2005). The dynamin-related GTPases have been shown to have central roles in the fusion-fission dynamics of mammalian mitochondria. The mitofusins (MFNs) are proteins localized at the mitochondrial outer membrane that are required for the fusion of mitochondria (Santel, 2006), whereas OPA1 in the inner membrane mediates the fusion (Olichon et al., 2006). The key component of the fission machinery is dynamin-related protein 1 (Drp1) (Labrousse et al., 1999; Smirnova et al., 2001).

Dysfunction of mitochondria is highly connected to neurodegenerative diseases, and abrogation of the fusion machinery is an early and causal event in neurodegeneration (Chan, 2006a; Knott et al., 2008; Lin and Beal, 2006). Mutations in *MFN2* cause the autosomal dominant disease Charcot-Marie-Tooth (CMT) type 2A, a peripheral neuropathy of long motor and sensory neurons; and Purkinje neurons in the mouse model have aberrant mitochondrial distribution, ultrastructure and electron transport activity (Chen et al., 2007; Santel, 2006; Zuchner et al., 2004). Mutations in *OPA1* cause autosomal dominant optic atrophy (ADOA), the most commonly inherited form of optic nerve degeneration (Alexander et al., 2000; Delettre et al., 2000; Olichon et al., 2006). However, it is still largely unknown as to how the abnormal mitochondrial morphology leads to neurodegenerative disorders.

Other consequences of impaired mitochondrial fusion-fission dynamics in the nervous system model have also been studied. In *Drosophila*, observation of *opa1* and *drp1* mutants has revealed impaired mitochondrial fusion-fission dynamics in the nervous system. An eye-specific homozygous mutation of *opa1* causes rough and glossy eye phenotypes in adult flies, suggesting that an increase in apoptosis is occurring (Yarosh et al., 2008). Mutations in *drp1* result in elongated mitochondria that are mostly absent from the presynapses (Verstreken et al., 2005). It has been reported that dendritic mitochondria are more metabolically active than axonal mitochondria (Overly et al., 1996) and that the dendritic distribution of mitochondria and their activity are essential and limiting for the development and morphological plasticity of dendritic spines in cultured hippocampal neurons (Li et al., 2004). In *Drosophila* loss of mitochondrial complex II activity causes degeneration of photoreceptors and disruption of mitochondrial protein translation severely affects the maintenance of terminal arborization of dendrites (Chihara et al., 2007; Mast et al., 2008). Nevertheless, it is not yet well understood how proper mitochondrial morphology, distribution and activity contribute to the formation and maintenance of dendritic arbors.

[1]Graduate School of Biostudies, Kyoto University, Yoshida Konoe-cho, Sakyo-ku, Kyoto 606-8507, Japan. [2]Graduate School of Medicine, Kyoto University, Yoshida Konoe-cho, Sakyo-ku, Kyoto 606-8507, Japan. [3]Department of Biological Sciences, Tokyo Metropolitan University, 1-1 Minami-osawa, Hachioji-shi, Tokyo, 192-0397, Japan.

*Present address: Graduate School of Biostudies, Kyoto University, South Campus Research Building (Building G), Kyoto University, Yoshida Konoe-cho, Sakyo-ku, Kyoto 606-8507, Japan
[†]Author for correspondence (tauemura@lif.kyoto-u.ac.jp)

Accepted 8 September 2009

Here, we addressed this question by using *Drosophila* dendritic arborization (da) neurons. Individually identified da neurons are classified into classes I-IV in order of increasing field size and arbor complexity, and they produce dendritic arbors of stereotypic patterns in a two-dimensional manner between the epidermis and muscles (Grueber et al., 2002; Orgogozo and Grueber, 2005; Sugimura et al., 2003).

Here, we show that Preli (protein of relevant evolutionary and lymphoid interest)-like (Prel), a *Drosophila* mitochondrial protein of the conserved PRELI/MSF1 family (Dee and Moffat, 2005), contributes to the integrity of mitochondrial structure and activity, and to the morphogenesis of dendritic arbors. Mutant *prel* class IV neurons simplified and downsized their dendritic arbors, and showed breakages of their major branches without detectable signs of apoptosis. Furthermore, we observed genetic interactions between Prel and the *Drosophila* Bax-like Bcl-2 family proteins Drob-1 (also known as Debcl) and Buffy (Colussi et al., 2000; Igaki et al., 2000; Quinn et al., 2003). All of these observations suggest that Prel-dependent control of mitochondrial activity has a pivotal role in the development and maintenance of dendritic arbors.

MATERIALS AND METHODS

Drosophila strains

We used the Gal4-UAS system (Brand and Perrimon, 1993) to express transgenes and to visualize da neurons. Gal4 lines used were $Gal4^{NP0738}$ (Hayashi et al., 2002), $Gal4^{ppk}$ (Ainsley et al., 2003), $Gal4^{109(2)80}$ (Gao et al., 1999), $Gal4^{2\text{-}21}$ (Grueber et al., 2003) and $Gal4^{elav[c155]}$. UAS marker fly stocks were provided from the Bloomington Stock Center or the *Drosophila* Genetic Resource Center at the Kyoto Institute of Technology. *UAS-drob-1/debcl/dBrog-1/dBok* (Senoo-Matsuda et al., 2005), *UAS-dronc [DN]* (Quinn et al., 2000), *UAS-p35* (Yoo et al., 2002) and *UAS-Buffy/Drob2* (Quinn et al., 2003) were gifts from M. Miura (University of Tokyo, Japan). The *milt* mutant strain was $milt^{[92]}/CyO$ (Stowers et al., 2002).

GS screening and isolation of *prel* mutant

To identify genes causing abnormal dendritic patterns, we adopted the P-element-based gene search (GS) system (Toba et al., 1999). For the screening, female flies that expressed $Gal4^{ppk}$ *UAS-mCD8::GFP* were crossed to the male flies of individual GS lines to induce overexpression of GS-vector flanking sequences in F1 progeny. Out of 3000 GS lines screened, we found that 47 lines showed abnormal dendrite phenotypes; analysis of insertion sites in individual lines led to identification of 27 candidate genes. Another overexpression screening was recently reported for the da neuron (Ou et al., 2008), and our screening rediscovered six genes (*hdc*, *spen*, *pnt*, *HmgD*, *foxo* and *lola*) that these authors had reported to cause dendrite phenotypes.

Molecular cloning

To identify *prel* mutations, we isolated genomic DNA from the wild-type flies (+/+) or heterozygous flies of 56 jump-out stocks that were homozygous lethal. Then, we identified the 1452 bp deletion including the *prel* ORF region by using genomic PCR and sequencing (Fig. 3A). Both *prel* and *opa1* cDNA were synthesized from embryos (5-20 hours AEL) by using Ready-To-Go RT-PCR Beads (Amersham Pharmacia) and primers that were designed on the basis of the wild-type gene sequences in FlyBase (http://flybase.bio.indiana.edu). To construct pUAST-mito::tdTomato, we assembled the cDNA fragment of human cytochrome c oxidase subunit 8A gene of pCAG-mito::VENUS (Okita et al., 2004), tdTomato of pRSET-tdTomato (Shaner et al., 2004) and pUAST (Brand and Perrimon, 1993). For the construction of *prel*-GAL4, the 2-kbp upstream sequence of the *prel* coding region was inserted into pPTGAL4 (Sharma et al., 2002). pUAST-HA::Drob-1 (Senoo-Matsuda et al., 2005) was a gift from M. Miura, and pUAST-Myc::Buffy/Drob2 was donated by T. Igaki (Kobe University, Japan). dsRNAs for the dynamin-related domain of *opa1*, full-length of *prel* and EGFP were synthesized by using a MEGAscript kit (Ambion).

MARCM analysis, image acquisition and quantification of dendritic trees

MARCM analysis and time-lapse recordings were performed basically as described previously (Lee and Luo, 1999; Satoh et al., 2008). To acquire images of da neurons in adults, we removed the heads, wings and legs of adult flies and mounted the abdomens in 90% glycerol. All of the images of da neurons, except for those of immunostaining of Fig. S2 and Fig. S3E-S3G in the supplementary material, were acquired from whole-mounted live larvae or from the adult abdomens by using a Zeiss LSM 510 META laser-scanning confocal microscopy system. For quantification of dendritic patterns of da neurons, we used Neurocyte software (Kurabo). MetaMorph software (Molecular Devices) was used to estimate the amount of fluorescent mito::GFP signals (Satoh et al., 2008). Mitochondrial signal index is indicated as mitochondrial signal (pixel) divided by the total length of neuronal processes (μm).

Antibodies, RNAi, subcellular fractionation, immunoblotting and assays of ATP levels and enzymatic activities

GST fusion proteins of *Drosophila* Prel and Opa1 were expressed and used for generating rat antibodies. For RNAi experiments S2 cells were cultured with 20 μg/ml dsRNA of the full-length *prel* or GFP-coding sequence. For DNA transfection we used Nucleofector R and its reagent (Amaxa). The mitochondrial fraction of S2 cells was prepared by using a Qproteome Mitochondria Isolation Kit (Qiagen). For immunoblotting, we used anti-HA antibody 16B12 (Covance), anti-α-tubulin antibody DM1A Ab (Sigma) and anti-Complex-V α-subunit antibody 15H4C4 (Invitrogen). The basic methods for assays of ATP levels and enzymatic activities were described previously (Senoo-Matsuda et al., 2005; Trounce et al., 1996).

Light and electron microscopy

S2 cells were seeded into concanavalin-A-coated glass-bottomed culture dishes, incubated with Mitotracker Orange (Invitrogen), and then fixed for immunostaining. Mitochondrial membrane potential was analyzed by using tetramethylrosamine methyl ester (TMRM; Invitrogen). For EM, fixed S2 cells were embedded in Epon812 (Nacalai Tesque) to prepare ultrathin sections. For immuno-EM of S2 cells, prepared ultrathin sections were exposed to mouse anti-HA antibody 16B12 (Covance). After washing with PBS, the grids were incubated with anti-IgG antibody that had been conjugated with 18 nm gold particles (Jackson ImmunoResearch) and stained with uranyl acetate and lead citrate. All of the EM specimens were examined with an H-7650 transmission electron microscope (Hitachi) operating at 80 kV. Detailed information of all of the methods will be promptly provided upon request.

RESULTS

Prel is a *Drosophila* mitochondrial protein of the Preli/MSF1 family and required for shaping filamentous mitochondria in S2 cells

We conducted a screening by using the Gene Search (GS) system to hunt for genes that control complex morphology of dendritic arbors of the class IV neuron at larval stages. One of the aims of this system is to drive overexpression or misexpression of genes neighboring the GS-vector insertion site (Toba et al., 1999). Out of 3000 GS lines screened, we focused on one of the GS lines, *GS9160*, and its candidate gene, *preli-like* (*prel*), which is conserved throughout eukaryotes. The predicted product of *prel* is 236 amino acids in length and a member of the PRELI/MSF1 family in *Drosophila* (Dee and Moffat, 2005). The closest human homolog is PRELI; and its amino acid sequence shows 46% identity to that of Preli-like through the entire length In yeast, Ups1p, a member of this family, is localized in mitochondria and regulates their shape (Sesaki et al., 2006). To confirm whether the Prel protein is localized to mitochondria in *Drosophila* cells, we fractionated lysates of *Drosophila* Schneider 2 (S2) cells and showed that both endogenous and exogenously expressed Prel proteins were predominantly

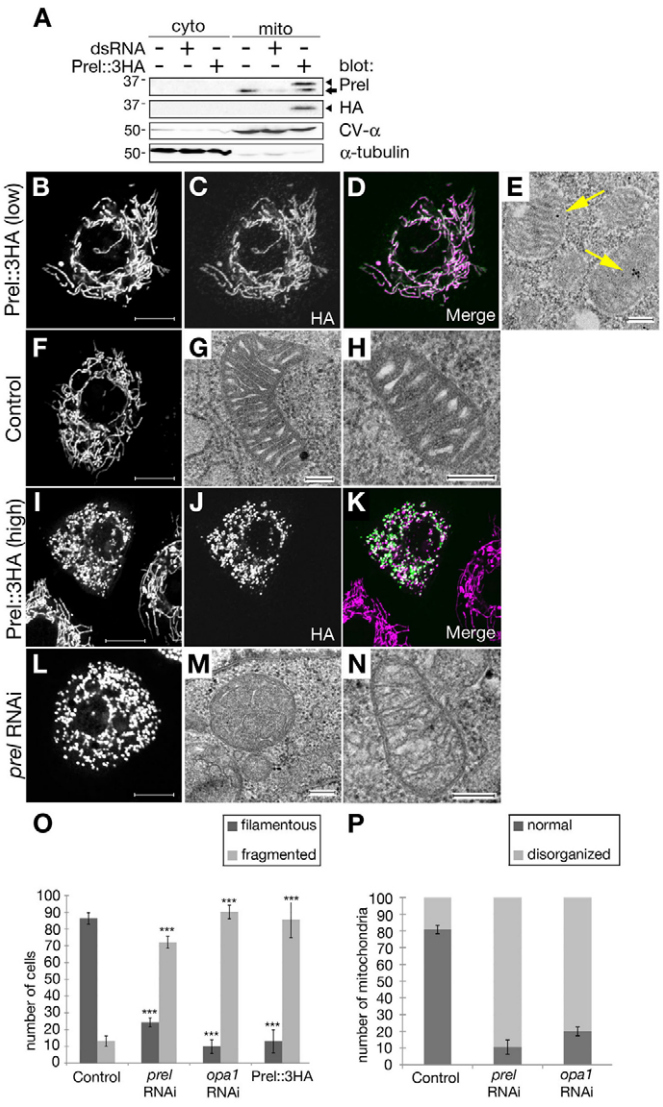

Fig. 1. Prel is a mitochondrial protein and its knockdown affects mitochondrial morphology of S2 cells. (**A**) Western blot analysis of Prel in S2 cells. Individual proteins were detected by the antibodies listed on the right. α-tubulin and CV-α, a component of mitochondrial F1F0 ATP synthase, are loading controls for cytoplasmic and mitochondrial proteins, respectively. Endogenous Prel and exogenously expressed Prel::3HA are indicated by the arrow and arrowhead, respectively. cyto, cytoplasmic fraction; mito, mitochondrion-enriched fraction. (**B-N**) Light micrographs of S2 cells (B-D,F,I-L) and ultrastructure of mitochondria in S2 cells (E,G,H,M,N). In the light micrographs (except for C and J), mitochondria were visualized by using Mitotracker Orange. (F-H) *EGFP* dsRNA-treated S2 cells as a control. (B-D,I-K) Prel::3HA-expressing S2 cells were stained with Mitotracker Orange (B,I) and for HA (C,J). The expression level was lower in B-D than in I-K: signal intensity of Prel::3HA in I-K was five times higher than in B-D. (E) Localization of Prel::3HA in mitochondria is shown by immunoelectron microscopy (yellow arrows). (L-N) *prel*-knockdown cells. Scale bars: 10 μm in B-D,F,I-L; 200 nm in E,G,H,M,N. (**O**,**P**) Quantification of mitochondrial morphology in *EGFP* dsRNA-treated cells as a control, in *prel*- or *opa1*-knockdown cells, and in Prel::3HA-expressing cells. Evaluation was made on the basis of light micrographs of S2 cells (O) and ultrastructure of mitochondria in S2 cells (P). (P) Mitochondria that have an abnormally expanded matrix (M) and/or only a few thin cristae (N) were defined as disorganized mitochondria. Data are presented as mean ± s.d. of three independent sets of experiments. ***P<0.001 (one-way analysis of variance between groups (ANOVA) with Tukey's HSD post-hoc analysis).

detected in the mitochondria-enriched fraction but hardly found in the cytoplasm (Fig. 1A). Under the light microscope, the expressed Prel was mostly colocalized with the mitochondrial marker Mitotracker Orange (Fig. 1B-D), and it appeared to be associated with the cristae when observed by immunoelectron microscopy (Fig. 1E).

By both light and transmission electron microscopy, we examined the role of Prel in shaping mitochondria in S2 cells. More than 80% of the control S2 cells had a filamentous mitochondrial network (Fig. 1F,O), and parallel, accordion-like folds of cristae structures were observed in each mitochondrion (Fig. 1G,H,P). Both knockdown of *prel* and its exogenous expression caused significant fragmentation of mitochondria (Fig. 1I-L,O). At the ultrastructural level, *prel*-knockdown cells had many mitochondria with lower electron density. Those mitochondria took on a round shape, having an abnormally expanded matrix (Fig. 1M) and only a few thin cristae (Fig. 1N). It is known that OPA1, one of the mitochondrial dynamin-related GTPases, is important for both fusion of inner membranes and maintenance of the structure of cristae (Chan, 2006b; Cipolat et al., 2006; Frezza et al., 2006; Meeusen et al., 2006; Okamoto and Shaw, 2005). We showed that knockdown of *opa1* in S2 cells affected the mitochondrial structure in a very similar manner to that found with knockdown of *prel* (Fig. 1O,P; see Fig. S1 in the supplementary material).

Both *prel* knockdown and its exogenous expression reduce mitochondrial activity in S2 cells

It is well known that the mitochondrial oxidative phosphorylation activity in cultured mammalian cells reflects mitochondrial shape and generates an electrochemical proton gradient across the mitochondrial inner membrane (Yaffe, 1999). To study whether *prel* knockdown affected mitochondrial activity in live S2 cells, we used tetramethylrosamine methyl ester (TMRM) to detect the mitochondrial membrane potential. Quantitative comparisons of the membrane potential showed that *prel* knockdown significantly reduced this potential when compared with the potential of control healthy cells (Fig. 2A). We also analyzed the ATP level as an indicator of mitochondrial metabolism and showed that knockdown of either *prel* or *opa1* and overexpression of *prel* reduced the ATP level (Fig. 2B), although the effects were less severe than the acute one caused by treating the cells with hydrogen peroxide or the protonophore carbonyl cyanide m-chlorophenylhydrazone (CCCP) (Fig. 2A,B). We also measured mitochondrial respiratory chain enzyme activities in *prel*-knockdown cells. The enzymatic activity of neither rotenone-sensitive NADH-cytochrome *c* oxidoreductase (an indicator of complex I and II) nor antimycin-A-sensitive succinate-cytochrome *c* oxidoreductase (complex II and III) was affected, whereas KCN-sensitive cytochrome *c* oxidase activity (complex IV) was decreased in *prel*-knockdown cells (Fig. 2C-E). All of these results suggest that *prel* knockdown or its expression beyond the physiological level not only had deleterious effects on the morphology but also on the activity of the mitochondria.

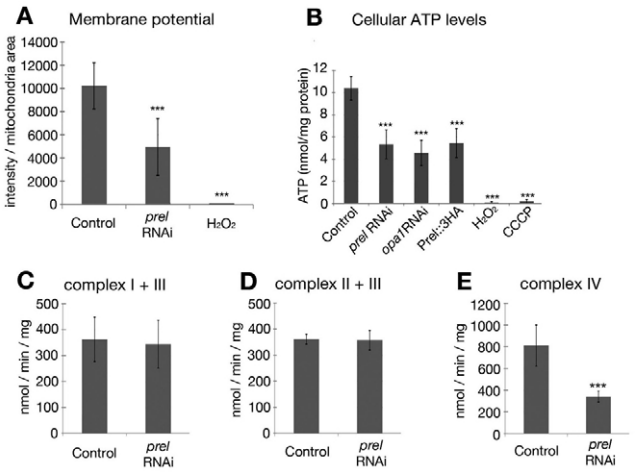

Fig. 2. Prel affects mitochondrial activity in S2 cells. (**A**) Quantitative comparisons of mitochondrial membrane potential. The membrane potential is indicated by the TMRM intensity. The fluorescence intensity of 100 cells was measured under each condition. (**B**) Quantitative comparisons of the cellular ATP content. Cells were treated for 5 days with dsRNA of either *EGFP*, *prel* or *opa1*, for 30 minutes with hydrogen peroxide or for 4 hours with carbonyl cyanide m-chlorophenylhydrazone (CCCP), a protonophore. (**C-E**) Mitochondrial respiratory chain enzymatic activities. (C) Complex I+III activity (rotenone-sensitive NADH-cytochrome c oxidoreductase). (D) Complex II+III activity (antimycin A-sensitive succinate-cytochrome c oxidoreductase). (E) Complex IV activity (KCN-sensitive cytochrome *c* oxidase). The data are presented as mean ± s.d. of three independent experiments; ***P<0.001 (ANOVA with Tukey's HSD post-hoc analysis).

Both *prel* loss-of-function and its overexpression cause mislocalization and fragmentation of mitochondria in class IV neurons

prel mRNA was found to be ubiquitously distributed in the embryo till stage 17 (data not shown). We observed that *prel* was expressed in class IV da neurons by using two *Gal4* lines that were expected to trap an enhancer region of *prel* (see Fig. S2A-F in the supplementary material). To study phenotypes of the loss of *prel* function, we remobilized the GS vector of *GS14515* and isolated a deletion (designated $prel^{1}$ or simply *prel* hereafter) that almost totally lacked the open reading frame (Fig. 3A). $prel^{1}$ homozygous mutants were lethal at early larval stages before their dendritic patterns became mature, and this lethality was recovered by broad expression of Prel::3HA by using a *daughterless* (*da*)-*GAL4* driver. To study how loss of *prel* function would affect mitochondria and dendrite morphogenesis of class IV neurons at the later, third-instar stages of larval development (4-5 days after egg laying), we generated and labeled *prel* mutant clones in heterozygous mature larvae by using a mosaic analysis in this and subsequent experiments (Lee and Luo, 1999). Throughout this study, we visualized mitochondria in da neurons by expressing fluorescent proteins that were tagged with a mitochondrial targeting signal, such as mito::GFP (Verstreken et al., 2005), and dendritic branches with membrane-bound fluorescent proteins. All of the images of larval da neurons, except for those of immunostaining of Fig. S2 and Fig. S4E-G in the supplementary material, were acquired from whole-mounted live larvae.

Mitochondria were distributed in cell bodies, axons and dendrites in control class IV neurons (Fig. 3B,C,F,G); and our quantification showed that mito::GFP signals were more numerous in axons than

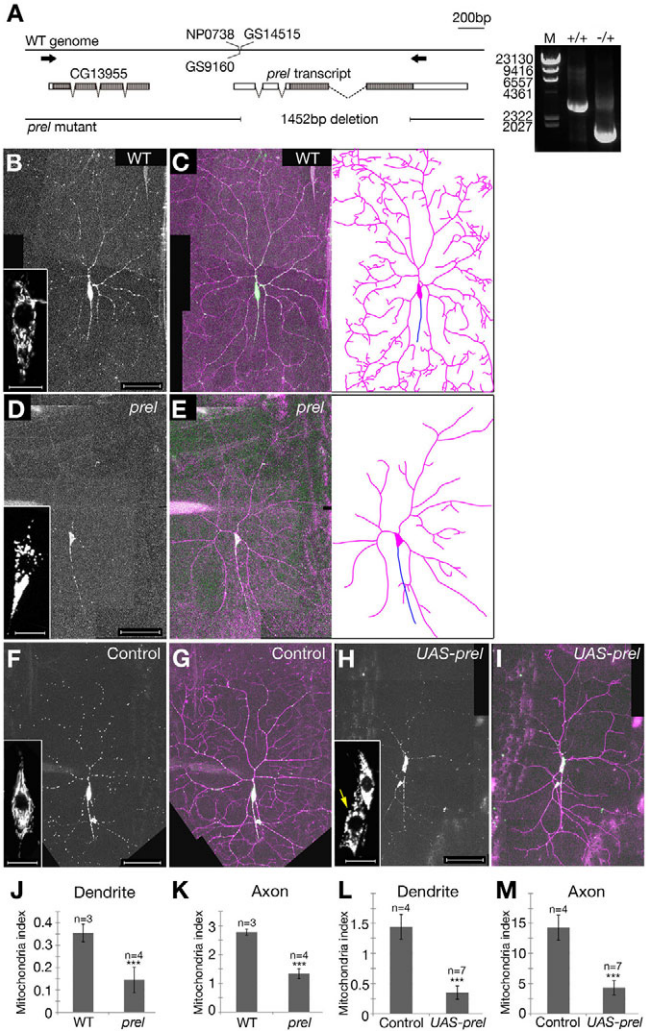

Fig. 3. Both *prel* loss-of-function and overexpression causes mislocalization and fragmentation of mitochondria in class IV neurons. (**A**) The exon-intron structure of *prel*, P-element insertion sites and the *prel* deletion mutant. White boxes represent untranslated regions (UTRs), and cross-hatched boxes are protein-coding regions. *NP0738*, *GS9160* and *GS14515* strains have P-element insertions in the 5′ UTR. Genomic organization of the *prel* allele was characterized by PCR using a pair of primers (arrows). Amplified fragments of *yw* (+/+) and heterozygous *prel* (–/+) of adult flies are shown. (**B-I**) Distribution of mitochondria in ddaC neurons. Mitochondria were visualized with mito::GFP (B,D,F,H; green in C,E,G,I) and neuronal plasma membranes were labeled with myr::mRFP (magenta in C,E,G,I). (Insets in B,D,F,H) High-magnification images of cell bodies. The yellow arrow in H indicates a ddaC neuron. (B-E) Clones of the wild-type (B,C) and *prel* (D,E). (F-I) Control ddaC (F,G) and ddaC-overexpressing Prel::3HA (H,I). Tracings of axons (blue) and dendritic arbors (magenta) of representative wild-type (C) and *prel* (E) clones are shown to the right of the merged images. All images were taken at the third-instar larval stage; dorsal is to the top and anterior is to the left. Detailed genotypes of the animals and clones imaged in all figures can be provided upon request. Scale bars: 100 μm in B,D,F,H; 10 μm in insets of B,D,F,H. (J-M) Quantification of mitochondrial signals in both dendrites (J,L) and axons (K,M). (**J**,**K**) Clones of the wild-type (WT) and *prel* (*prel*). (**L**,**M**) Control ddaC (Control) and ddaC-overexpressing Prel::3HA (*UAS-prel*). In this and all subsequent graphs, numbers of neurons analyzed are indicated above individual bars, unless described otherwise. Data are presented as mean ± s.d. ***P<0.001 for each value compared with control neurons by Student's *t*-test.

in dendrites by an order of magnitude (WT and control in Fig. 3J-M). The distribution of mitochondria in dendrites was not necessarily restricted to branching points. The density of the mitochondrial signals was significantly reduced in both axons and dendrites either in *prel* mutant neurons or in the wild-type background neurons overexpressing *prel* (Fig. 3D,E,H,I; *prel* and UAS-*prel* in Fig. 3J-M). We found a filamentous mitochondrial network in cell bodies of the control neurons (insets of Fig. 3B,F); by contrast, both *prel* loss-of-function and *prel* overexpression appeared to cause fragmentation of mitochondria (insets of Fig. 3D,H). All of these results suggest that *prel* was necessary for proper mitochondrial distribution in neuronal processes and the tubular morphology in class IV da neurons.

Dysfunction of *prel* causes simplification, downsizing and local breakage of dendritic arbors of class IV neurons

Loss of *prel* function and its overexpression affected not only the subcellular distribution and shape of mitochondria in da neurons, but also the complex dendrite morphogenesis of class IV neurons. In contrast to the complicated and expansive dendritic arbors of the control neurons (Fig. 4A), those of the *prel* mutant neurons exhibited shorter, smaller, much less-branched dendritic arbors (Fig. 4B,C). A closer look at the distal regions of the mutant dendritic arbors showed that the terminal branches tended to be shorter than those of the wild-type neurons, making the mutant distal dendrites appear fuzzy. Strikingly, arbors of 9 out of 21 *prel* neurons had been locally destroyed, as judged by the presence of detached branches nearby (Fig. 4C and 4C′; see also Fig. S3A-B′ in the supplementary material). To examine whether there was a hot spot for this destruction, we plotted the spatial distribution of breakpoints in the mutant arbors (Fig. S3C in the supplementary material). The wild-type class IV neuron ddaC develops its receptive field with a radius of about 400 μm, whereas the radius of the mutant arbor was reduced to about 300 μm. Of the 55 breakage points examined, 22 were located within a 100 μm radius; and 51 out of 55 were within a 200 μm radius (see Fig. S3C in the supplementary material). This quantification showed that *prel* loss-of-function caused branch breakages more in the proximal area of the arbor than in the distal one. In contrast to this arbor destruction, we observed no axonal breakage, at least not close to the cell body, in any of the 21 mutant neurons observed.

These phenotypes of the mutant neurons were indeed due to loss of *prel* function, as shown by the fact that they were rescued to normal when a *prel* transgene was expressed (Fig. 4D). Overexpression of *prel* in the wild-type neurons also simplified and downsized their dendritic arbors (Fig. 4E). All of the above phenotypes were shown to be statistically significant by our quantification (Fig. 4F,G). It should be noted that we found no apoptotic signs in the *prel* mutant class IV neurons at the stage examined (see Fig. S4 in the supplementary material), making the possibility that the dendritic phenotype was a secondary consequence in dying cells less likely. In contrast to the effects on dendritic arbors of class IV neurons, those of class I-III appeared to be hardly affected by loss of *prel* function or *prel* overexpression (see Fig. S5 in the supplementary material).

The dendritic phenotype of *prel* mutant neurons is much more severe than that of *milt* mutant neurons

As described above, the *prel* mutant class IV neurons showed two classes of mitochondrial phenotypes: a reduction in mitochondrial signals in both dendrites and axons; and fragmentation in the cell body, which presumably decreased mitochondrial activity. We attempted to clarify cause-and-effect relationships between each of these mitochondrial phenotypes and the malformation of the dendritic arbor. To understand effects of the localization on dendrite morphogenesis, we examined how dendritic morphology was affected when the transport of mitochondria was blocked by using a loss-of-function mutation of *milton* (*milt*). Milt is an adaptor protein between mitochondria and kinesin and is required for mitochondrial transport in photoreceptor axons (Glater et al., 2006; Stowers et al., 2002) and in oocytes (Cox and Spradling, 2006). Milt was expressed

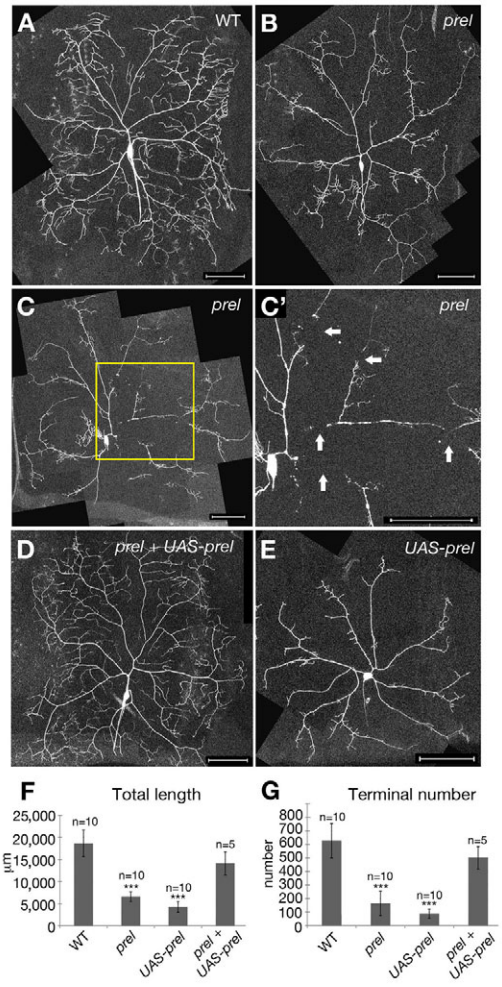

Fig. 4. Both *prel* loss-of-function and its overexpression cause a decrease in the total length and in the terminal numbers of class IV ddaC neurons. (**A-E**) Dendritic arbors of representative class IV ddaC neurons of the wild-type clone (A), *prel* mutant clone (B,C), the *prel* mutant clone expressing Prel::3HA (D), and the wild-type expressing Prel::3HA (E). (C′) High-magnification image of the box in C. Branches of the *prel* mutant neuron have broken and become detached from the dendritic arbor (arrows in C′). Labeled neurons (except those in E) are clones of MARCM analysis. Scale bars: 100 μm. (**F**,**G**) Quantification of total length of dendritic branches (F) and the number of terminal branches (G) of wild-type ddaC clones (WT), *prel* mutant clones (*prel*), *prel* mutant clones expressing Prel::3HA (*prel* + *UAS-prel*) and Prel::3HA-expressing neurons (*UAS-prel*) are shown. Broken branches of *prel* mutant clones were included in the quantification. Data are presented as mean ± s.d. ***$P<0.001$ (ANOVA with Tukey's HSD post-hoc analysis).

in da neurons in wild-type larvae (see Fig. S2G-I in the supplementary material). In *milt* mutant class IV neurons, mitochondria were hardly distributed in dendrites or axons, as we had expected (Fig. 5A,C,E,F). In contrast to this strong mislocalization phenotype, abnormalities of dendritic arbors of the *milt* mutant neurons were substantially milder than those of the *prel* neurons (Fig. 5B,D,G,H). These results imply that a reduction in mitochondrial signals in dendrites and axons might per se not lead to severe morphological abnormalities of dendritic arbors.

Dendritic phenotypes caused by overexpression of Drob-1, a *Drosophila* Bcl-2 family protein, are reminiscent of those of *prel* mutant neurons

We then explored the relationship between alterations of mitochondrial activity and dendrite morphogenesis. For this purpose, we investigated previously isolated genes that control mitochondrial membrane structure and activity, including a *Drosophila* protein of the Bcl-2 family, Drob-1 (also known as Debcl) (Colussi et al., 2000; Igaki et al., 2000). It is known that members of the mammalian Bcl-2 family control permeabilization of mitochondrial outer membrane in apoptotic cells and also are involved in mitochondrial respiration (Danial et al., 2003; Karbowski et al., 2006; Youle and Strasser, 2008). As described later, we found that overexpression of *prel* or *drob-1* decreased ATP levels in neurons, suggesting impaired mitochondrial function. This overexpression of Drob-1 caused simplification and downsizing of dendritic arbors of class IV neurons and, in addition, breakage of proximal branches (Fig. 6A,E,F). Of the 20 neurons examined, arbors of four neurons had such breakages. The overexpression also resulted in a decrease in mitochondrial density in neuronal processes (Fig. 6C,D,G), all of which were similar to those of *prel* mutant neurons (Fig. 3D,E,H,I; Fig. 4B,C).

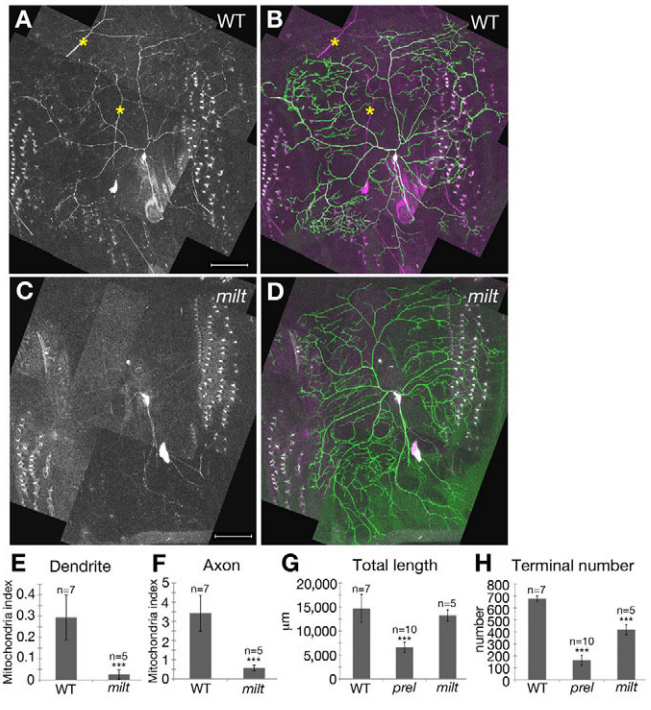

Fig. 5. Mitochondrial distribution and dendritic pattern of *milton* (*milt*) mutant class IV neurons. (**A-D**) Distribution of mitochondria in ddaC clones of the wild-type (A,B) and *milt* (C,D). Mitochondria were visualized with mito::tdTomato (A,C; magenta in B,D) and the neuronal plasma membrane was labeled with mCD8::GFP (green in B,D). Asterisks indicate auto-fluorescent signals of the trachea. Scale bars: 100 μm. (**E**,**F**) Quantification of mitochondrial signals in both dendrite (E) and axon (F) of clones of the wild-type (WT) and *milt* (*milt*). Data are presented as mean ± s.d. ***P<0.001 for each value compared with the wild-type neurons by Student's t-test. (**G**,**H**) Quantification of total length of dendritic branches (G) and the number of terminal branches (H) of individual wild-type ddaC clones (WT), *prel* mutant clones (*prel*), and *milt* mutant clones (*milt*). Data are presented as mean ± s.d. ***P<0.001 (ANOVA with Tukey's HSD post-hoc analysis).

Expression of Drob-1 antagonist Buffy in *prel* mutant neurons restores their dendritic morphology

The above results suggest that *prel* dysfunction or *drob-1* overexpression resulted in the malformation of dendritic arbors, primarily by way of reducing mitochondrial activity. It has been shown that Buffy, another fly Bcl-2 family protein, acts as a Drob-1 antagonist in photoreceptor cells (Quinn et al., 2003). Consistent with the antagonistic molecular function of Buffy, the *drob-1*-overexpression phenotype was suppressed by co-overexpressing *buffy*. Overexpression of *buffy* alone hardly affected dendrite morphogenesis or mitochondrial distribution (Fig. 6E-G; see Fig. S6 in the supplementary material). Based on these observations, we addressed whether expression of Buffy might suppress the assumed reduction in the mitochondrial activity of the *prel* mutant class IV neurons and consequently restore its dendrite phenotype. We found that the abnormal morphology of dendritic arbors of the *prel* neurons was remarkably recovered to normal when the *buffy* transgene was expressed (Fig. 6B), and there were no significant differences between dendritic arbors of the wild-type neurons and those of *prel* mutant neurons expressing *buffy* on the basis of either of the two parameters examined (Fig. 6E,F). All of these results suggest that the aberrant dendritic arbors of the *prel* neurons are mostly due to mitochondrial dysfunction.

Progressive regression of dendritic arbors when *prel* function is impaired in larval and adult neurons

Loss-of-function mutations in the genes controlling mitochondrial fusion, such as *MFN2* and *OPA1*, are associated with neurodegenerative diseases (Chan, 2006a; Knott et al., 2008); however, it has not been reported that mutations of the human *prel* gene are linked to any of these diseases. To investigate whether dysfunction of *prel* in mitochondria elicits late-onset neurodegeneration, we observed class IV neurons in larvae and adults.

We performed time-lapse recordings of dendritic arbors of *prel* mutant class IV neurons from an early second-instar stage until the mature late third-instar stage (see Figs S7 and S8 in the supplementary material). In the wild-type neuron, the dendritic arbor elaborated terminal branches (see Fig. S7 in the supplementary material). By contrast, terminal branches of the mutant neurons were eliminated, and major branches became almost bald over this time period (see Fig. S8 in the supplementary material). This time-lapse analysis, together with the 'local destruction' phenotype, indicates that intact mitochondrial function prevented both of the two modes of dendrite regression: the breakage of proximal branches and the retraction of terminal branches.

Dramatic remodeling of dendritic arbors occurs in da neurons undergoing metamorphosis (Kuo et al., 2005; Williams and Truman, 2005). Two out of the three class IV neurons in each abdominal

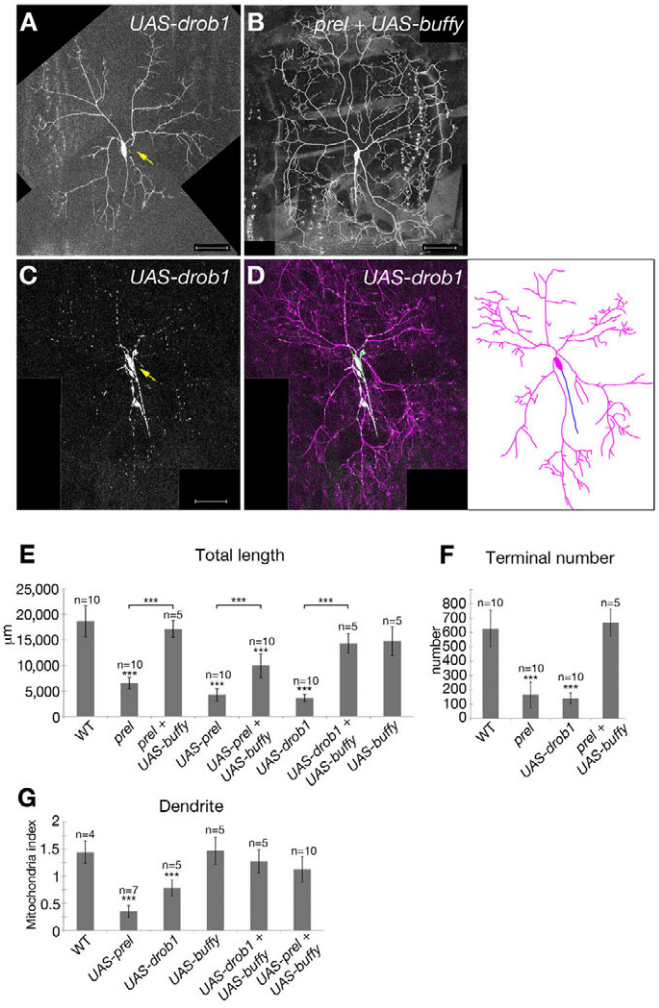

Fig. 6. Expression of Drob-1, a *Drosophila* Bcl-2 family member, affects dendritic pattern formation of class IV neurons. (**A-D**) Dendritic arbors and mitochondrial distribution of representative class IV ddaC neurons of the wild-type overexpressing *drob-1* (A,C,D) and the *prel* mutant clone overexpressing *buffy* (B). (A) The primary branch was severed in the proximal region of the arbor of the *drob-1*-overexpressed neuron shown (yellow arrow in A). The *prel* mutant phenotype could be rescued to normal by overexpression of *buffy* (B). The mitochondria were visualized with mito::GFP (C; green in D); and the neuronal plasma membrane was labeled with myr::mRFP (magenta in D). The yellow arrow in C indicates a ddaC neuron. Tracings of the axon (blue) and the dendritic arbor (magenta) of the *drob-1*-overexpressed neuron (D) are shown at the right of the merged image. Scale bars: 100 μm. (**E**,**F**) Quantification of total length of dendritic branches (E) and the number of terminal branches (F) of wild-type ddaC clones (WT), *prel* mutant clones (*prel*), *prel* mutant clones that overexpressed *buffy* (*prel* + *UAS-buffy*), *prel*-overexpressing neurons (*UAS-prel*), neurons that coexpressed *prel* and *buffy* (*UAS-prel* + *UAS-buffy*), *drob-1*-overexpressing neurons (*UAS-drob1*), neurons that coexpressed *drob-1* and *buffy* (*UAS-drob1* + *UAS-buffy*), and *buffy*-overexpressing neurons (*UAS-buffy*). (**G**) Quantification of mitochondrial signals in dendrites of control ddaC neurons (*Gal4^{ppk} UAS-myr::mRFP UAS-mito::GFP*) (WT), and those of ddaC overexpressing either *prel* (*UAS-prel*), *prel* and *buffy* (*UAS-prel* + *UAS-buffy*), *drob-1* (*UAS-drob1*), *drob-1* and *Buffy* (*UAS-prel* + *UAS-buffy*) or *buffy* (*UAS-Buffy*). Data are presented as mean ± s.d. ***P<0.001 and **P<0.01 (ANOVA with Tukey's HSD post-hoc analysis).

hemisegment survive metamorphosis and remodel their dendritic arbors (Kuo et al., 2005; Shimono et al., 2009). One of those two, v'ada, developed an arbor with a lattice pattern in the lateral plate of the adult control abdomen, which persisted throughout adult life (Fig. 7A-C,H) (Shimono et al., 2009). In contrast to that of the wild-type neurons, the total length of dendritic branches of *prel*-overexpressing neurons was significantly decreased; and those neurons displayed late-onset retraction of their arbors when observed at 10 and 30 days as adults (Fig. 7D,E,H). Overexpression of Drob-1 also led to retraction, with a similar time course (Fig. 7F,G,H). Moreover we observed *prel* mutant clones of v'ada in adults at different ages and acquired images suggesting that their dendritic branches had progressively retracted (Fig. 7I-K). We found that ATP levels in heads of adult flies that overexpressed *prel* or *drob-1* under a pan-neuronal driver were significantly lower than those in control flies, suggesting an impaired mitochondrial function (Fig. 7L). These reductions in the ATP level were restored by co-expressing *buffy*, exactly as were the abnormal dendritic morphologies. These results strongly suggest that Prel-dependent mitochondrial function is essential for maturation and maintenance of dendritic trees throughout the life of *Drosophila*.

DISCUSSION

The molecular function of Prel

We showed that both *prel* loss-of-function and its overexpression abrogated mitochondrial structures and activity in S2 cells and also in da neurons. Apparently an appropriate expression level of Prel is required for controlling mitochondrial shape, structure of the cristae, the activity of respiratory chain complex IV and the cellular ATP level. What then is the exact molecular function of Prel?

The molecular function of the Preli family is largely unknown in multicellular organisms. It has been recently shown that Ups1p, the yeast homologue of Prel, regulates the level of cardiolipin (CL), a phospholipid of mitochondrial membranes (Osman et al., 2009; Tamura et al., 2009). CL is known to be located predominantly in the mitochondria and has diverse mitochondrial functions including stabilization of the respiratory chain supercomplex (Joshi et al., 2009). These reports imply that the reduction in the complex IV activity and the ATP level in the *prel*-knockdown cells could be attributed to the altered phospholipid composition. Further biochemical study is required to measure the complex IV activity and phospholipid composition in various genetic backgrounds including Buffy or Drob1 overexpression, which might help to find evidence for a molecular pathway that includes Prel and Buffy.

However, it has been also proposed that loss of Ups1p affects the function of the yeast OPA1 homolog Mgm1p, which is important for both fusion of inner membranes and maintenance of the structure of the cristae (Chan, 2006b; Cipolat et al., 2006; Frezza et al., 2006; Meeusen et al., 2006; Okamoto and Shaw, 2005). Mgm1p is imported into mitochondria, and its function is regulated by proteolytic cleavage (Griparic et al., 2007; McQuibban et al., 2003; Song et al., 2007; Tamura et al., 2009). This import and cleavage pattern is altered, and the mitochondria fragmented, in the yeast *ups1p* mutant (Sesaki et al., 2006; Tamura et al., 2009). We showed that the knockdown of *Drosophila opa1* in S2 cells affected the structure and activity of mitochondria similarly to *prel* knockdown, suggesting that *Drosophila* Prel is also required for organizing the mitochondrial inner membrane structure in concert with *Drosophila* Opa1. However, we could not provide positive evidence for any functional linkage between these two molecules. Neither *prel* knockdown nor its overexpression strongly affected the cleavage pattern of endogenous Opa1 in S2 cells (data not shown). A better

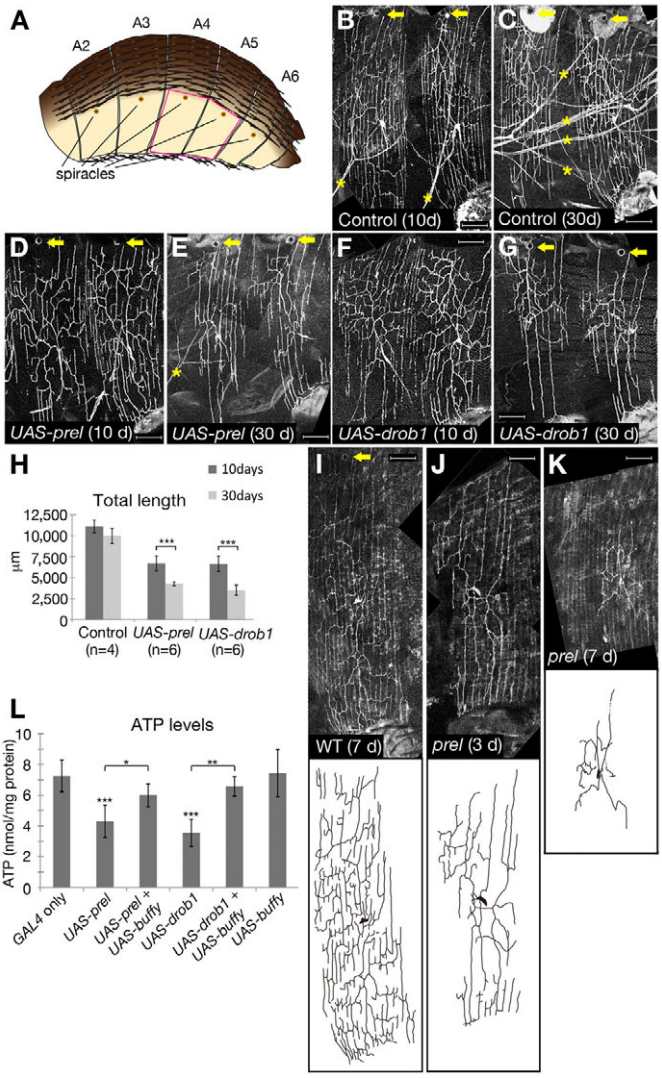

Fig. 7. Progressive simplification of dendritic arbors of neurons overexpressing *prel* or *drob-1* in adults. (**A**) Illustration of the lateral view of the adult abdomen. (**B-G**) Class IV v'ada neurons that have undergone dendritic remodeling in metamorphosis. Control neurons (B,C), neurons overexpressing Prel::3HA (D,E) and those overexpressing Drob-1 (F,G) are shown. Images are abdominal hemisegments A4 and A5 of adult flies at 10 days (B,D,F) or 30 days (C,E,G) after eclosion. Asterisks indicate autofluorescent signals of the trachea. (**H**) Quantification of total length of dendritic branches of control neurons (Control), Prel::3HA-overexpressing neurons (*UAS-prel*) and Drob-1-overexpressing neurons (*UAS-drob-1*). Data are presented as mean ± s.d. ***P<0.001 for each value compared with the neurons at 10 days after eclosion by Student's t-test. (**I-K**) Dendritic arbors of representative v'ada clones of the wild type at 7 days after eclosion (I), *prel* at 3 days after eclosion (J) and *prel* at 7 days after eclosion (K). Tracings of dendritic arbors of individual neurons are shown at the bottom of the raw images. In B-G and I, yellow arrows indicate spiracles as landmarks. The number of clones obtained was: three WT, four *prel* 3d and four *prel* 7d. Scale bars: 100 µm in B-G,I-K. (**L**) ATP levels in *elav-GAL4/+* (*GAL4* only), *UAS-prel::3HA/+; elav-GAL4/+* (*UAS-prel*), *UAS-prel::3HA UAS-buffy/+; elav-GAL4/+* (*UAS-prel + UAS-buffy*), *elav-GAL4/UAS-drob1* (*UAS-drob1*), *UAS-buffy/+; elav-GAL4/UAS-drob1* (*UAS-drob1 + UAS-buffy*), and *UAS-buffy/+; elav-GAL4/+* (*UAS-buffy*). The adult heads of each genotype were analyzed. Data are presented as mean ± s.d. ***P<0.001, **P<0.01 and *P<0.05 (ANOVA with Tukey's HSD post-hoc analysis).

understanding of Prel function in the protein import into mitochondria requires further study. It should be noted that there seems to be a bidirectional relationship between mitochondrial shape and bioenergetics, as suggested by the fact that a decrease in the ATP level can also stimulate mitochondrial fragmentation (Knott et al., 2008). One possible interpretation of our data might be that Prel is primarily required for maintaining the normal level of intracellular ATP and controls mitochondrial shape indirectly.

Effects of mitochondrial dysfunction on different classes of neurons

Mitochondria are abundant in regions of intense energy consumption, such as muscles, sperm and neurons; and OPA1 expression is high in the retina, brain, testis, heart and skeletal muscle (Alexander et al., 2000). The CMT type 2A phenotype due to *MFN2* mutations might reflect the extreme cell geometry, as shown by the fact that long peripheral nerves are particularly sensitive to perturbations produced by MFN2-mediated mitochondrial dysfunction (Santel, 2006). Class IV neurons, which develop expansive and complicated dendritic arbors, probably consume the highest amount of ATP; thus they are very vulnerable to a loss or reduction in the *prel*-dependent mitochondrial function. The differential Gal4 expression of the trap line and the *cis*-element fusion line suggests that Prel is expressed most strongly in class IV neurons among the four subclasses (see Fig. S2 in the supplementary material).

Abnormal mitochondrial distribution is not necessarily linked to the severe morphological defect of the dendritic arbor

We had speculated that the severe dendritic phenotype of the *prel* class IV neurons could be primarily due to the misdistribution of mitochondria. However, our attempts to correlate the mitochondrial localization and the dendritic phenotype suggested that such a view might be naive. Loss of function of *milt* dramatically reduced the mitochondrial density in neuronal processes; nevertheless, the dendritic phenotype of the *milt* mutant neuron was much less profound than that of the *prel* neurons. Similarly, *milt* mutant eyes are indistinguishable from the wild-type eyes in their external and photoreceptor morphology in spite of the paucity of mitochondria in photoreceptor axon terminals (Stowers et al., 2002). These observations imply the possibility that the visible misdistribution of mitochondria per se might not necessarily lead to the severe morphological abnormality of dendritic arbors or axons.

How can we interpret these observations? Overexpression of *prel* diminished the ATP level in vivo, where the local ATP concentration within the cell might fall below a threshold that is necessary for dendritic growth and maintenance. However, mitochondria that remain in the cell body of the *milt* neuron might maintain their ATP-producing activity, and at least a subpopulation of synthesized ATP molecules might diffuse a long distance to reach the distal region in the dendritic arbor. These hypotheses would be testable if the ATP level in the cell body and its diffusion inside dendritic branches could be visualized and measured quantitatively in various genetic backgrounds (Imamura et al., 2009).

Prel-dependent control of mitochondrial activity prevents regression of dendritic branches

Dysfunction of mitochondria correlates with neurodegenerative diseases and is an early and causal event in neurodegeneration (Chan, 2006a; Knott et al., 2008; Lin and Beal, 2006). The results of this study imply that the evolutionally conserved Prel might prevent

neurodegeneration in other animal species, as discussed below. When Prel function was impaired, branches in the proximal region of the arbor were degraded, and terminal branches were eliminated at the mature larval stage; and in adult flies, overall arbors retracted. These phenotypes are reminiscent of breakage of neurite branches within and near amyloid deposits in the brain of a transgenic mouse model of Alzheimer disease, which is speculated to occur through mitochondrial dysfunction, oxidative stress and calcium deregulation (Tsai et al., 2004). The branch destruction of the *prel* mutant neuron could also be due to a 'physical' reason. Transport of various cargos might be impaired when ATP is limited, leading to a defect in mechanical strength of the membrane. Such fragile branches could be ruptured during larval locomotion.

It has been intensively studied whether the mutant proteins that are associated with hereditary neurodegenerative diseases affect mitochondrial function. Our study has provided cellular and genetic evidence that Prel is a novel target of such research. Future studies should be directed towards further characterization of the Prel protein by using both fly and vertebrate systems to clarify its function in mitochondria and its involvement in mechanisms that prevent the regression of dendritic arbors.

Acknowledgements

The antibodies and fly stocks were provided by the Developmental Studies Hybridoma Bank at the University of Iowa, the Bloomington Stock Center and the *Drosophila* Genetic Resource Center at Kyoto Institute of Technology. We thank Yuh-Nung Jan for communicating data before publication. We are also grateful to M. Miura, T. Igaki, L. Luo, Y. N. Jan, T. Schwarz, T. Schroeder, Y. Hiromi and A. Kadota for other fly strains and materials. We thank M. Miura, H. Chihara, M. Yamamoto, Y. Kozutsumi and A. Kawaguchi for their technical advice and/or discussion; S. Yonehara for use of the DNA sequencer and Multilabel Counter; and K. Shimizu and M. Futamata for their technical assistance. This work was supported by grants from the programs Grants-in-Aid for Scientific Research on Priority Areas Molecular Brain Science (17024025 to T.U.) and Systems Genomics (17017032 to T.A.). A.T. and T.T. are recipients of a fellowship of the Japan Society for the Promotion of Science.

Supplementary material

Supplementary material for this article is available at
http://dev.biologists.org/cgi/content/full/136/22/3757/DC1

References

Ainsley, J. A., Pettus, J. M., Bosenko, D., Gerstein, C. E., Zinkevich, N., Anderson, M. G., Adams, C. M., Welsh, M. J. and Johnson, W. A. (2003). Enhanced locomotion caused by loss of the Drosophila DEG/ENaC protein Pickpocket1. *Curr. Biol.* **13**, 1557-1563.

Alexander, C., Votruba, M., Pesch, U. E., Thiselton, D. L., Mayer, S., Moore, A., Rodriguez, M., Kellner, U., Leo-Kottler, B., Auburger, G. et al. (2000). OPA1, encoding a dynamin-related GTPase, is mutated in autosomal dominant optic atrophy linked to chromosome 3q28. *Nat. Genet.* **26**, 211-215.

Brand, A. H. and Perrimon, N. (1993). Targeted gene expression as a means of altering cell fates and generating dominant phenotypes. *Development* **118**, 401-415.

Chan, D. C. (2006a). Mitochondria: Dynamic organelles in disease, aging, and development. *Cell* **125**, 1241-1252.

Chan, D. C. (2006b). Mitochondrial fusion and fission in mammals. *Annu. Rev. Cell Dev. Biol.* **22**, 79-99.

Chen, H., McCaffery, J. M. and Chan, D. C. (2007). Mitochondrial fusion protects against neurodegeneration in the cerebellum. *Cell* **130**, 548-562.

Chihara, T., Luginbuhl, D. and Luo, L. (2007). Cytoplasmic and mitochondrial protein translation in axonal and dendritic terminal arborization. *Nat. Neurosci.* **10**, 828-837.

Cipolat, S., Rudka, T., Hartmann, D., Costa, V., Serneels, L., Craessaerts, K., Metzger, K., Frezza, C., Annaert, W., D'Adamio, L. et al. (2006). Mitochondrial rhomboid PARL regulates cytochrome c release during apoptosis via OPA1-dependent cristae remodeling. *Cell* **126**, 163-175.

Colussi, P. A., Quinn, L. M., Huang, D. C., Coombe, M., Read, S. H., Richardson, H. and Kumar, S. (2000). Debcl, a proapoptotic Bcl-2 homologue, is a component of the Drosophila melanogaster cell death machinery. *J. Cell Biol.* **148**, 703-714.

Cox, R. T. and Spradling, A. C. (2006). Milton controls the early acquisition of mitochondria by Drosophila oocytes. *Development* **133**, 3371-3377.

Danial, N. N., Gramm, C. F., Scorrano, L., Zhang, C. Y., Krauss, S., Ranger, A. M., Datta, S. R., Greenberg, M. E., Licklider, L. J., Lowell, B. B. et al. (2003). BAD and glucokinase reside in a mitochondrial complex that integrates glycolysis and apoptosis. *Nature* **424**, 952-956.

Dee, C. T. and Moffat, K. G. (2005). A novel family of mitochondrial proteins is represented by the Drosophila genes slmo, preli-like and real-time. *Dev. Genes Evol.* **215**, 248-254.

Delettre, C., Lenaers, G., Griffoin, J. M., Gigarel, N., Lorenzo, C., Belenguer, P., Pelloquin, L., Grosgeorge, J., Turc-Carel, C., Perret, E. et al. (2000). Nuclear gene OPA1, encoding a mitochondrial dynamin-related protein, is mutated in dominant optic atrophy. *Nat. Genet.* **26**, 207-210.

Detmer, S. A. and Chan, D. C. (2007). Functions and dysfunctions of mitochondrial dynamics. *Nat. Rev. Mol. Cell Biol.* **8**, 870-879.

Frezza, C., Cipolat, S., Martins de Brito, O., Micaroni, M., Beznoussenko, G. V., Rudka, T., Bartoli, D., Polishuck, R. S., Danial, N. N., De Strooper, B. et al. (2006). OPA1 controls apoptotic cristae remodeling independently from mitochondrial fusion. *Cell* **126**, 177-189.

Gao, F. B., Brenman, J. E., Jan, L. Y. and Jan, Y. N. (1999). Genes regulating dendritic outgrowth, branching, and routing in Drosophila. *Genes Dev.* **13**, 2549-2561.

Glater, E. E., Megeath, L. J., Stowers, R. S. and Schwarz, T. L. (2006). Axonal transport of mitochondria requires milton to recruit kinesin heavy chain and is light chain independent. *J. Cell Biol.* **173**, 545-557.

Griparic, L., Kanazawa, T. and van der Bliek, A. M. (2007). Regulation of the mitochondrial dynamin-like protein Opa1 by proteolytic cleavage. *J. Cell Biol.* **178**, 757-764.

Grueber, W. B., Jan, L. Y. and Jan, Y. N. (2002). Tiling of the Drosophila epidermis by multidendritic sensory neurons. *Development* **129**, 2867-2878.

Grueber, W. B., Jan, L. Y. and Jan, Y. N. (2003). Different levels of the homeodomain protein cut regulate distinct dendrite branching patterns of Drosophila multidendritic neurons. *Cell* **112**, 805-818.

Hayashi, S., Ito, K., Sado, Y., Taniguchi, M., Akimoto, A., Takeuchi, H., Aigaki, T., Matsuzaki, F., Nakagoshi, H., Tanimura, T. et al. (2002). GETDB, a database compiling expression patterns and molecular locations of a collection of Gal4 enhancer traps. *Genesis* **34**, 58-61.

Igaki, T., Kanuka, H., Inohara, N., Sawamoto, K., Nunez, G., Okano, H. and Miura, M. (2000). Drob-1, a Drosophila member of the Bcl-2/CED-9 family that promotes cell death. *Proc. Natl. Acad. Sci. USA* **97**, 662-667.

Imamura, H., Huynh Nhat, K. P., Togawa, H., Saito, K., Iino, R., Kato-Yamada, Y., Nagai, T., Noji, H. (2009). Visualization of ATP levels inside single living cells with fluorescence resonance energy transfer-based genetically encoded indicators. *Proc. Natl. Acad. Sci. USA* (in press).

Joshi, A. S., Zhou, J., Gohil, V. M., Chen, S. and Greenberg, M. L. (2009). Cellular functions of cardiolipin in yeast. *Biochim. Biophys. Acta* **1793**, 212-218.

Karbowski, M., Norris, K. L., Cleland, M. M., Jeong, S. Y. and Youle, R. J. (2006). Role of Bax and Bak in mitochondrial morphogenesis. *Nature* **443**, 658-662.

Knott, A. B., Perkins, G., Schwarzenbacher, R. and Bossy-Wetzel, E. (2008). Mitochondrial fragmentation in neurodegeneration. *Nat. Rev. Neurosci.* **9**, 505-518.

Kuo, C. T., Jan, L. Y. and Jan, Y. N. (2005). Dendrite-specific remodeling of Drosophila sensory neurons requires matrix metalloproteases, ubiquitin-proteasome, and ecdysone signaling. *Proc. Natl. Acad. Sci. USA* **102**, 15230-15235.

Labrousse, A. M., Zappaterra, M. D., Rube, D. A. and van der Bliek, A. M. (1999). C. elegans dynamin-related protein DRP-1 controls severing of the mitochondrial outer membrane. *Mol. Cell* **4**, 815-826.

Lee, T. and Luo, L. (1999). Mosaic analysis with a repressible cell marker for studies of gene function in neuronal morphogenesis. *Neuron* **22**, 451-461.

Li, Z., Okamoto, K., Hayashi, Y. and Sheng, M. (2004). The importance of dendritic mitochondria in the morphogenesis and plasticity of spines and synapses. *Cell* **119**, 873-887.

Lin, M. T. and Beal, M. F. (2006). Mitochondrial dysfunction and oxidative stress in neurodegenerative diseases. *Nature* **443**, 787-795.

Mast, J. D., Tomalty, K. M., Vogel, H. and Clandinin, T. R. (2008). Reactive oxygen species act remotely to cause synapse loss in a Drosophila model of developmental mitochondrial encephalopathy. *Development* **135**, 2669-2679.

McQuibban, G. A., Saurya, S. and Freeman, M. (2003). Mitochondrial membrane remodelling regulated by a conserved rhomboid protease. *Nature* **423**, 537-541.

Meeusen, S., DeVay, R., Block, J., Cassidy-Stone, A., Wayson, S., McCaffery, J. M. and Nunnari, J. (2006). Mitochondrial inner-membrane fusion and crista maintenance requires the dynamin-related GTPase Mgm1. *Cell* **127**, 383-395.

Okamoto, K. and Shaw, J. M. (2005). Mitochondrial morphology and dynamics in yeast and multicellular eukaryotes. *Annu. Rev. Genet.* **39**, 503-536.

Okita, C., Sato, M. and Schroeder, T. (2004). Generation of optimized yellow and red fluorescent proteins with distinct subcellular localization. *Biotechniques* **36**, 418-422, 424.

Olichon, A., Guillou, E., Delettre, C., Landes, T., Arnaune-Pelloquin, L., Emorine, L. J., Mils, V., Daloyau, M., Hamel, C., Amati-Bonneau, P. et al. (2006). Mitochondrial dynamics and disease, OPA1. *Biochim. Biophys. Acta* **1763**, 500-509.
Orgogozo, V. and Grueber, W. B. (2005). FlyPNS, a database of the Drosophila embryonic and larval peripheral nervous system. *BMC Dev. Biol.* **5**, 4.
Osman, C., Haag, M., Potting, C., Rodenfels, J., Dip, P. V., Wieland, F. T., Brugger, B., Westermann, B. and Langer, T. (2009). The genetic interactome of prohibitins: coordinated control of cardiolipin and phosphatidylethanolamine by conserved regulators in mitochondria. *J. Cell Biol.* **184**, 583-596.
Ou, Y., Chwalla, B., Landgraf, M. and van Meyel, D. J. (2008). Identification of genes influencing dendrite morphogenesis in developing peripheral sensory and central motor neurons. *Neural Dev.* **3**, 16.
Overly, C. C., Rieff, H. I. and Hollenbeck, P. J. (1996). Organelle motility and metabolism in axons vs dendrites of cultured hippocampal neurons. *J. Cell Sci.* **109**, 971-980.
Quinn, L., Coombe, M., Mills, K., Daish, T., Colussi, P., Kumar, S. and Richardson, H. (2003). Buffy, a Drosophila Bcl-2 protein, has anti-apoptotic and cell cycle inhibitory functions. *EMBO J.* **22**, 3568-3579.
Quinn, L. M., Dorstyn, L., Mills, K., Colussi, P. A., Chen, P., Coombe, M., Abrams, J., Kumar, S. and Richardson, H. (2000). An essential role for the caspase dronc in developmentally programmed cell death in Drosophila. *J. Biol. Chem.* **275**, 40416-40424.
Santel, A. (2006). Get the balance right: mitofusins roles in health and disease. *Biochim. Biophys. Acta* **1763**, 490-499.
Satoh, D., Sato, D., Tsuyama, T., Saito, M., Ohkura, H., Rolls, M. M., Ishikawa, F. and Uemura, T. (2008). Spatial control of branching within dendritic arbors by dynein-dependent transport of Rab5-endosomes. *Nat. Cell Biol.* **10**, 1164-1171.
Senoo-Matsuda, N., Igaki, T. and Miura, M. (2005). Bax-like protein Drob-1 protects neurons from expanded polyglutamine-induced toxicity in Drosophila. *EMBO J.* **24**, 2700-2713.
Sesaki, H., Dunn, C. D., Iijima, M., Shepard, K. A., Yaffe, M. P., Machamer, C. E. and Jensen, R. E. (2006). Ups1p, a conserved intermembrane space protein, regulates mitochondrial shape and alternative topogenesis of Mgm1p. *J. Cell Biol.* **173**, 651-658.
Shaner, N. C., Campbell, R. E., Steinbach, P. A., Giepmans, B. N., Palmer, A. E. and Tsien, R. Y. (2004). Improved monomeric red, orange and yellow fluorescent proteins derived from Discosoma sp. red fluorescent protein. *Nat. Biotechnol.* **22**, 1567-1572.
Sharma, Y., Cheung, U., Larsen, E. W. and Eberl, D. F. (2002). PPTGAL, a convenient Gal4 P-element vector for testing expression of enhancer fragments in drosophila. *Genesis* **34**, 115-118.
Shimono, K., Fujimoto, A., Tsuyama, T., Yamamoto-Kochi, M., Sato, M., Hattori, Y. Sugimura, K., Usui, T., Kimura, K., and Uemura, T. (2009). Multidendritic sensory neurons in the adult Drosophila abdomen: origins, dendritic morphology, and segment- and age-dependent programmed cell death. *Neural Dev.* **4**, 37.
Smirnova, E., Griparic, L., Shurland, D. L. and van der Bliek, A. M. (2001). Dynamin-related protein Drp1 is required for mitochondrial division in mammalian cells. *Mol. Biol. Cell* **12**, 2245-2256.
Song, Z., Chen, H., Fiket, M., Alexander, C. and Chan, D. C. (2007). OPA1 processing controls mitochondrial fusion and is regulated by mRNA splicing, membrane potential, and Yme1L. *J. Cell Biol.* **178**, 749-755.
Stowers, R. S., Megeath, L. J., Gorska-Andrzejak, J., Meinertzhagen, I. A. and Schwarz, T. L. (2002). Axonal transport of mitochondria to synapses depends on milton, a novel Drosophila protein. *Neuron* **36**, 1063-1077.
Sugimura, K., Yamamoto, M., Niwa, R., Satoh, D., Goto, S., Taniguchi, M., Hayashi, S. and Uemura, T. (2003). Distinct developmental modes and lesion-induced reactions of dendrites of two classes of Drosophila sensory neurons. *J. Neurosci.* **23**, 3752-3760.
Tamura, Y., Endo, T., Iijima, M. and Sesaki, H. (2009). Ups1p and Ups2p antagonistically regulate cardiolipin metabolism in mitochondria. *J. Cell Biol.* **185**, 1029-1045.
Toba, G., Ohsako, T., Miyata, N., Ohtsuka, T., Seong, K. H. and Aigaki, T. (1999). The gene search system. A method for efficient detection and rapid molecular identification of genes in Drosophila melanogaster. *Genetics* **151**, 725-737.
Trounce, I. A., Kim, Y. L., Jun, A. S. and Wallace, D. C. (1996). Assessment of mitochondrial oxidative phosphorylation in patient muscle biopsies, lymphoblasts, and transmitochondrial cell lines. *Methods Enzymol.* **264**, 484-509.
Tsai, J., Grutzendler, J., Duff, K. and Gan, W. B. (2004). Fibrillar amyloid deposition leads to local synaptic abnormalities and breakage of neuronal branches. *Nat. Neurosci.* **7**, 1181-1183.
Verstreken, P., Ly, C. V., Venken, K. J., Koh, T. W., Zhou, Y. and Bellen, H. J. (2005). Synaptic mitochondria are critical for mobilization of reserve pool vesicles at Drosophila neuromuscular junctions. *Neuron* **47**, 365-378.
Williams, D. W. and Truman, J. W. (2005). Cellular mechanisms of dendrite pruning in Drosophila: insights from in vivo time-lapse of remodeling dendritic arborizing sensory neurons. *Development* **132**, 3631-3642.
Yaffe, M. P. (1999). The machinery of mitochondrial inheritance and behavior. *Science* **283**, 1493-1497.
Yarosh, W., Monserrate, J., Tong, J. J., Tse, S., Le P. K., Nguyen, K., Brachmann, C. B., Wallace, D. C. and Huang, T. (2008). The molecular mechanisms of OPA1-mediated optic atrophy in Drosophila model and prospects for antioxidant treatment. *PLoS Genet.* **4**, e6.
Yoo, S. J., Huh, J. R., Muro, I., Yu, H., Wang, L., Wang, S. L., Feldman, R. M., Clem, R. J., Muller, H. A. and Hay, B. A. (2002). Hid, Rpr and Grim negatively regulate DIAP1 levels through distinct mechanisms. *Nat. Cell Biol.* **4**, 416-424.
Youle, R. J. and Strasser, A. (2008). The BCL-2 protein family: opposing activities that mediate cell death. *Nat. Rev. Mol. Cell Biol.* **9**, 47-59.
Zuchner, S., Mersiyanova, I. V., Muglia, M., Bissar-Tadmouri, N., Rochelle, J., Dadali, E. L., Zappia, M., Nelis, E., Patitucci, A., Senderek, J. et al. (2004). Mutations in the mitochondrial GTPase mitofusin 2 cause Charcot-Marie-Tooth neuropathy type 2A. *Nat. Genet.* **36**, 449-451.